ELSEVIER

Thermochimica Acta 388 (2002) 343–354

thermochimica acta

www.elsevier.com/locate/tca

Non-isothermal curing of a diepoxide–cycloaliphatic diamine system by temperature modulated differential scanning calorimetry

S. Montserrat*, J.G. Martín

Departament de Màquines i Motors Tèrmics, Universitat Politècnica de Catalunya, Carrer de Colom 11, E-08222 Terrassa, Spain

Received 25 July 2001; received in revised form 9 December 2001; accepted 10 December 2001

Abstract

The non-isothermal curing of an epoxy resin based on diglycidyl ether of bisphenol A (DGEBA) with a diamine based on 3,3′-dimethyl-4,4′-diaminodicyclohexylmethane (3DCM) was analysed by temperature modulated differential scanning calorimetry (TMDSC). The TMDSC scans were performed at underlying heating rates, q_0, of between 1 and 0.1 K min^{-1}, and at the following modulation conditions: an amplitude of 0.2 K and a period of 60 s. For values of q_0 equal to or lower than 0.5 K min^{-1}, a vitrification and further devitrification of the system was observed in the modulus of the complex heat capacity, $|C_p^*|$, and also in the phase angle signal. Both the time and the temperature of vitrification and devitrification are used to construct a continuous heating transformation (CHT) cure diagram. This diagram was completed by the lines that give the evolution of the temperature and the glass transition temperature over time at constant heating rate. The effect of the steric hindrance of the diamine is analysed in the curing kinetics and the maximum glass transition temperature of the resin. The thermal stability of the reacting system was studied by thermogravimetric analysis.

Keywords: Temperature modulated DSC; Non-isothermal curing; Vitrification; Devitrification; Continuous heating transformation cure diagram

1. Introduction

In a previous paper, the thermal properties of the diepoxide–cycloaliphatic diamine and the kinetics of the curing reaction were studied by conventional differential scanning calorimetry (DSC) and temperature modulated DSC (TMDSC) [1]. In particular, TMDSC was used in the study of the vitrification of the system and the modelling of the overall kinetics, including the step controlled by diffusion. Under isothermal conditions, the vitrification of the reacting system takes place when the crosslinking of the network produces a resin in which the glass transition temperature equals the curing temperature. Similarly, in a system submitted to a constant heating rate, the vitrification takes place when the temperature of the system equals the glass transition temperature of the system. Conversely, the system undergoes devitrification when the temperature of the system becomes higher than the glass transition temperature.

Vitrification and devitrification processes during the non-isothermal curing of epoxy resins have been studied by Gillham and co-workers [2] and Wisanrakkit and Gillham [2,3] using torsional braid analysis

* Corresponding author. Tel.: +34-937-398-123; fax: +34-937-398-101.
E-mail address: montserrat@mmt.upc.es (S. Montserrat).

0040-6031/02/$ – see front matter
PII: S0040-6031(02)00019-9

(TBA), and DSC to determine the degree of conversion at which the relaxation occurs. Since the introduction of TMDSC by Reading [4], the curing of thermosets at a constant heating rate has been studied by employing this technique in other systems [5–10]. As is well known, TMDSC simultaneously gives the heat evolved during the curing and the heat capacity, allowing both the degree of conversion and the times at which vitrification and devitrification take place to be determined in the same experiment. This method has been used in the construction of the continuous heating transformation (CHT) cure diagram of epoxy resins [7,10].

In the present study, the non-isothermal curing of an epoxy resin based on diglycidyl ether of bisphenol A (DGEBA) with a diamine based on 3,3′-dimethyl-4,4′-diaminodicyclohexylmethane (3DCM) was analysed by temperature modulated DSC (TMDSC) at very low underlying heating rates, q_0. This diamine is relatively hindered and is thus chosen to obtain systems with longer pot life at room temperature [11]. The TMDSC technique was applied by the methodology of alternating DSC (ADSC, Mettler–Toledo), the main properties of which have been described elsewhere [1,12].

The effect of the heating rate on the temperature at which vitrification and further devitrification occurs was studied. These singular points were used to construct the CHT diagram, indicating the region in which the system vitrifies. The diagram was completed with the lines of T–t and T_g–t at a constant heating rate. The relation between the conversion degree and the glass transition temperature of the system allows the representation of the T_g–t lines. The crossing point between this line and the T–t line should give the referred points of vitrification and devitrification of the system at the respective heating rate. The deviations between the experimental and the calculated points is analysed.

2. Experimental

2.1. Materials

The resin was an epoxy based on DGEBA (Araldite LY564 from CIBA Speciality Chemicals), which was cured by a diamine based on 3DCM (HY 2954 from CIBA Speciality Chemicals). The epoxy equivalent of the resin was 170 g eq.$^{-1}$. The preparation of the samples was performed as described elsewhere [1].

2.2. Calorimetric measurements

The temperature modulated DSC measurements were performed with a Mettler–Toledo 821e thermoanalyser equipped with an intracooler. STAR© software was used for the evaluation of the ADSC curves. In the following sections of this study, we will refer to ADSC to indicate the TMDSC measurements. The temperature and heat flow calibrations were performed by standards of indium and zinc. The modulation conditions used in the non-isothermal ADSC experiments were of underlying heating rates of between 1 and 0.1 K min^{-1}, amplitudes of 0.2 or 0.5 K, and a period of 60 s, which was the same in all the experiments. In order to calibrate the heat flow signal, correct the amplitude and eliminate the cell asymmetry, ADSC needs to perform a blank with an empty pan on the reference side and an empty pan plus a lid on the sample side, at the same experimental parameters as in the sample measurement. For the ADSC measurements, the intrument constant τ_{lag} was set to 0.

The DSC scans required for the partial curing method were performed in the same instrument at a constant heating rate of 10 K min^{-1}. The sample weight was also approximately 8–10 mg. The nitrogen gas flow used in DSC and ADSC was 50 mL min^{-1}.

2.3. Thermogravimetric analysis

Loss of weight was measured using a Mettler–Toledo TG 50 thermogravimetric analyser at a temperature range of between 40 and 600 °C at heating rates of between 0.1 and 1 K min^{-1} and a nitrogen gas flow of 200 mL min^{-1}. The temperature scans were performed in samples of about 6 mg of the unreacted mixtures of epoxy and hardener.

3. Results and discussion

3.1. ADSC signals in non-isothermal curing

Firstly, we will show the generalised behaviour of the main ADSC signals in one non-isothermal curing experiment. The total heat flow, the modul us of the heat capacity and the phase angle obtained in the non-isothermal curing of the epoxy system at an

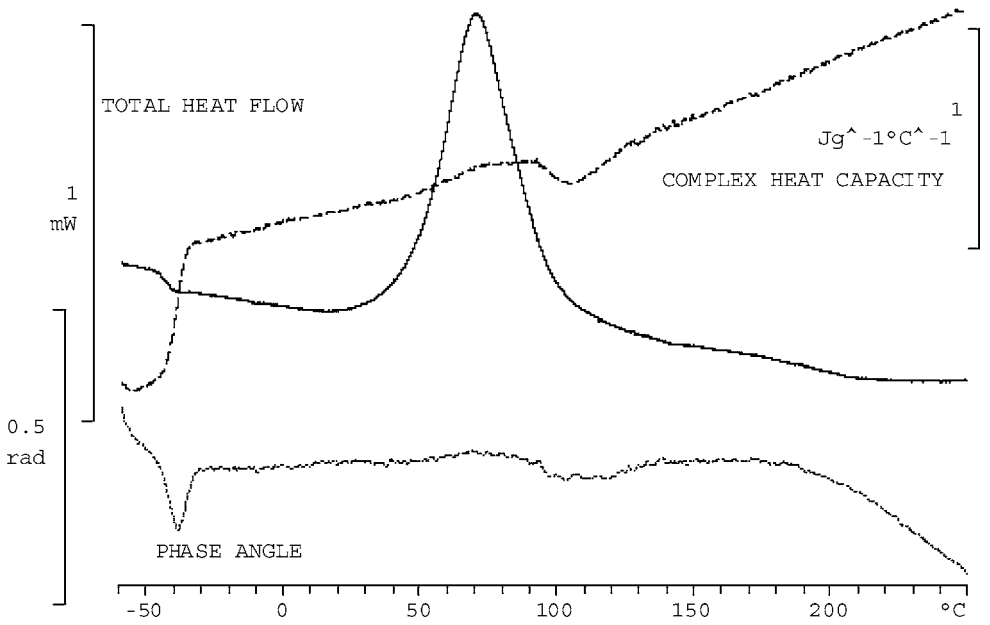

Fig. 1. Total heat flow (continuous line), complex heat capacity (dashed line) and phase angle (dotted line) signals of the non-isothermal cure of the epoxy-amine resin at an underlying heating rate of 0.4 K min^{-1}, an amplitude of 0.2 K and a period of 60 s.

underlying heating rate of 0.4 K min^{-1} and the modulation conditions of 0.2 K and 60 s are shown in Fig. 1. The total heat flow signal ($\langle\phi\rangle$) shows two thermal events. At low temperatures, this signal shows the glass transition of the unreacted resin, $T_{g0,\langle\phi\rangle}$, which is about −43 °C (measured as the midpoint of the glass transition) under these conditions. At increasing temperatures, the exothermic peak characteristic of the curing reaction is shown. The values of the heat of curing measured on the $\langle\phi\rangle$ signal ($\Delta H_{\langle\phi\rangle}$) is 473 J g^{-1}, which is slightly higher than the values measured by the conventional DSC (460 and 405 J g^{-1} at 2.5 and 20 K min^{-1}, respectively) [1].

The heat capacity signal, which is given by the modulus of the complex heat capacity, $|C_p^*|$, shows the thermal events related to the relaxation processes of the reacting system. The dynamic glass transition of the unreacted system, $T_{g0,|C_p^*|}$, is shown at a temperature of about −40 °C, which is slightly higher than the $T_{g0,\langle\phi\rangle}$ and is practically independent of the underlying heating rate according to the theoretical predictions [13,14]. After this glass transition, the $|C_p^*|$ increases in a quasi-linear manner with temperature, as expected, and a slight increase is observed in the region corresponding to the exothermic peak in the $\langle\phi\rangle$ signal. Increasing the temperature, at about 90 °C, there is a decrease in the $|C_p^*|$ signal, followed by an increase to about 110 °C. These variations of $|C_p^*|$ correspond to the vitrification and subsequent devitrification of the epoxy, respectively. In this epoxy resin, the vitrification process is sharper than the devitrification process, the midpoint vitrification temperature being 97 °C. Vitrification of the resin corresponds to the transition of the liquid state to the glassy state with a change in the degree of conversion from 0.84 to 0.90. As the temperature increases, in a wide temperature range, from 110 to about 131 °C, the system shows devitrification. A midpoint devitrification temperature of about 121 °C may be estimated. During the devitrification process, the resin changes from the glassy state to the liquid state and the degree of conversion increases to 0.95. In order to achieve full conversion, the epoxy must be heated to a temperature up to 250 °C.

These relaxation processes may also be recognised in the phase angle signal. At low temperatures, a sharp peak of relaxation shows the relaxation associated with the glass transition of the unreacted system ($T_{g0,\delta}$), whose value is shown in Table 1. A slight change in δ is observed coinciding with the maximum

Table 1
Glass transition temperature and variation of $|C_p^*|$ of the DGEBA–3DCM system[a]

q_0 (K min^{-1})	$T_{g0,\langle\phi\rangle}$ (°C)	$T_{g0,\lvert C_p^*\rvert}$ (°C)	$T_{g0,\delta}$ (°C)	$\Delta\lvert C_p^*\rvert(T_{g0})$ (J g^{-1} K^{-1})	$T_{g2s,\lvert C_p^*\rvert}$ (°C)	$\Delta\lvert C_p^*\rvert(T_{g2s})$ (J g^{-1} K^{-1})
1	−41.8	−40	−39	0.65	133.5[b]	–
0.5	−43.7	−40	−39	0.70	100.8[b]	–
0.4	−43.2	−40	−38.5	0.66	156.0	0.21
0.25	−41.6	−38	−37.1	0.69	159.2	0.23
0.1[c]	–	−40.4	−38.9	0.68	158.6	0.33
Average values	−42.5 ± 0.8	−39.6 ± 0.9	−38.5 ± 0.8	0.68 ± 0.02	157.9 ± 1.7	0.26 ± 0.06

[a] Glass transition temperatures of the unreacted system ($(T_{g0,\langle\phi\rangle}$, $T_{g0,|C_p^*|}$ and $T_{g0,\delta}$) and final T_g (T_{g2s}) from the second ADSC scan performed at the same underlying heating rate, and variation of $|C_p^*|$ at T_{g0} and T_{g2s}.

[b] Final T_g of samples submitted at temperatures higher than the onset temperature of thermal degradation. These values are not considered in the averaged value.

[c] The values at 0.1 K min^{-1} are an average of the two experiments.

of the exothermic reaction. Vitrification and devitrification are characterised by a broad peak, which includes both relaxation processes. At higher temperatures, a drift to increasing absolute values of δ is observed.

3.2. Heat of curing and degree of conversion

The total heat flow signals obtained during the curing at underlying heating rates of between 1 and 0.1 K min^{-1} are shown in Fig. 2. At 1 K min^{-1}, the $\langle\phi\rangle$ signal shows a main peak, as a result of the curing reaction. However, an additional quantity of heat is evolved between the end of the main peak, at 130–150 °C, and the final temperature of about 240 °C. At temperatures above 270 °C, a deviation from the base line is observed as a consequence of the thermal degradation of the sample.

The temperature of the main peak (T_p) decreases as the heating rate decreases. The ADSC values and those previously found by conventional DSC [1] may be fitted into a Kissinger plot ($\ln(qT_p^{-2})$ against T_p^{-1}) as shown in Fig. 3, the slope of which gives an apparent activation energy (E_a) of 58.7 kJ mol^{-1}. The slope of the fit with the ADSC values alone gives an $E_a = 60.2$ kJ mol^{-1}, which value agrees very well with the E_a of 58.7 kJ mol^{-1} calculated by conventional DSC [1].

As is usual, the measurement of the heat of curing is performed by the integration of the area under the heat flow signal, selecting a baseline, which in this study consisted of a straight line between the estimated temperatures at the beginning and the end of curing. The interval of temperatures was selected depending on the heating rate. This measurement gives an apparent heat of curing. Furthermore, the non-isothermal curing at a heating rate $q_0 \leq 0.5$ K min^{-1} shows the relaxation processes of vitrification and devitrification, which affect the heat capacity signal, as shown in Fig. 1 for $q_0 = 0.4$ K min^{-1}. As mentioned elsewhere [1,5,6,15], the heat flow measures the heat of reaction and the sensible heat due to the temperature dependence of the heat capacity. In order to measure the heat of reaction, free from the sensible heat, we use the so-called non-reversing heat flow, ϕ_{NR}. According to the approach introduced by Reading [4], ϕ_{NR} is defined as the difference between the total heat flow, $\langle\phi\rangle$, and the reversing heat flow, ϕ_R, which is given by the product $|C_p^*|q_0$, multiplied by -1 if the heat flow is recorded with the endothermic direction downwards, as in the present study. For q_0 of 1 and 0.5 K min^{-1} the values of ΔH_{NR} are practically the same as those of $\Delta H_{\langle\phi\rangle}$, but for lower q_0, ΔH_{NR} becomes smaller than $\Delta H_{\langle\phi\rangle}$, due to a more significant effect of the vitrification and the devitrification, which modifies the reversing heat flow signal. The variation of the degree of conversion (α) with the temperature for different heating rates was obtained by the non-reversing heat flow signal, using the values of ΔH_{NR}. The dependence of the heat of curing values (whether $\Delta H_{\langle\phi\rangle}$ or ΔH_{NR}) on the baseline and its limits, add some uncertainty to the calculations of the degree of conversion. Notwithstanding this experimental limitation, the values of the degree of conversion against the temperature are shown in Fig. 4.

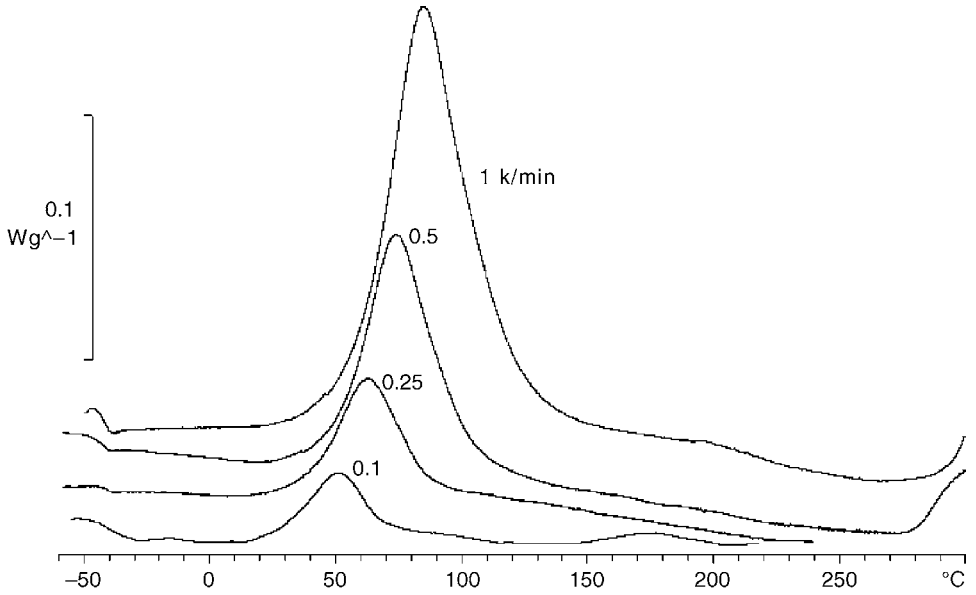

Fig. 2. Total heat flow signal of the curing of the DGEBA–3DCM system at underlying heating rates of between 0.1 and 1 K min^{-1}. Modulation conditions: an amplitude of 0.2 K and a period of 60 s. The scale of the specific heat flow is relative and the curves are shifted vertically for clarity.

A similar shape of the heat flow at $q_0 \geq 0.25$ K min^{-1} has also been observed in other epoxy resins studied by TMDSC (see Fig. 6 in [6], or Fig. 1 in [9]). The presence of this broad peak is attributed to the diffusion controlled regime, which may be detected in the $|C_p^*|$ signal. However, in the heat flow signal at 0.1 K min^{-1} a small second peak is observed. The reproducibility of this peak has been verified by curing fresh samples at the same experimental conditions, which results of the non-reversing heat flow and $|C_p^*|$ signal are shown in Fig. 5. As a consequence of this peak, the curve α–T at 0.1 K min^{-1} shows two steps (Fig. 4). The presence of this peak may be a consequence of the structure of the diamine and the chemical reactions of the system. The chemical structure of the 3DCM shows the methyl group in a neighbouring

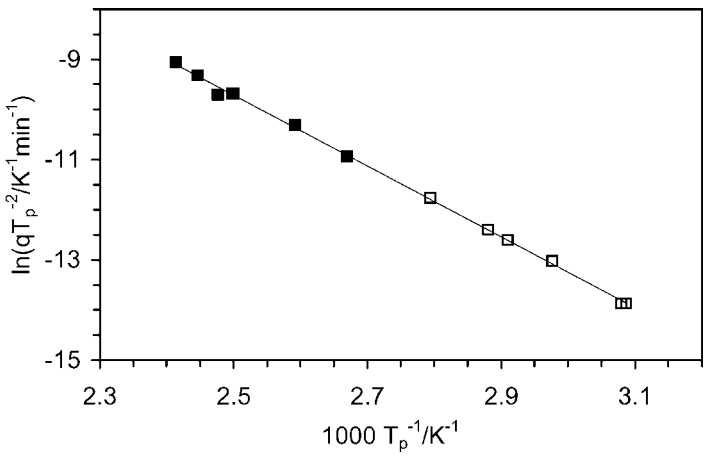

Fig. 3. Kissinger plot of the ADSC values (open squares) and DSC values (filled squares). The line is the linear fit to both sets of values.

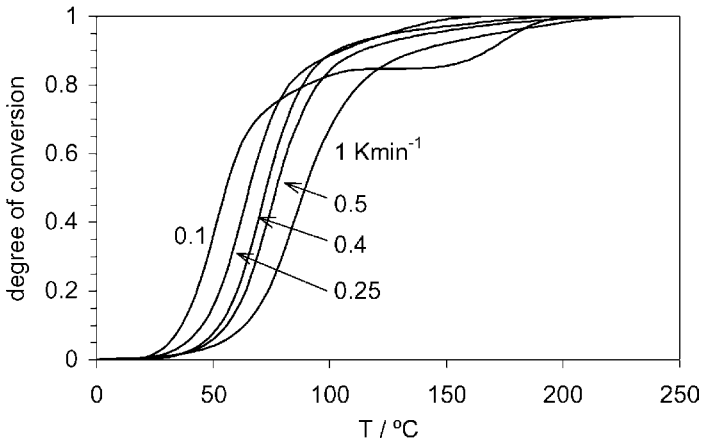

Fig. 4. Variation of the degree of curing on the temperature at underlying heating rates of between 0.1 and 1 K min^{-1}. The calculation of α was performed by the non-reversing heat flow signal.

position to the amine group [11,16], and this structure yields a steric hindrance that inhibits the reactivity of the amine groups. Nevertheless, at temperatures higher than 150 °C, where the system is not in the glassy state, a residual heat of curing originated by the unreacted amine groups may occur, increasing again the extent of reaction.

The effect of the steric hindrance is also shown in the measurement of the glass transition temperature T_g of the resin after a postcure reaction. The post cure of a sample isothermally cured at 160 °C for 10 min gives a T_g of 111 °C, with practically no residual heat of curing, when it is measured at 10 K min^{-1} by DSC. Nevertheless, when the temperature is increased to

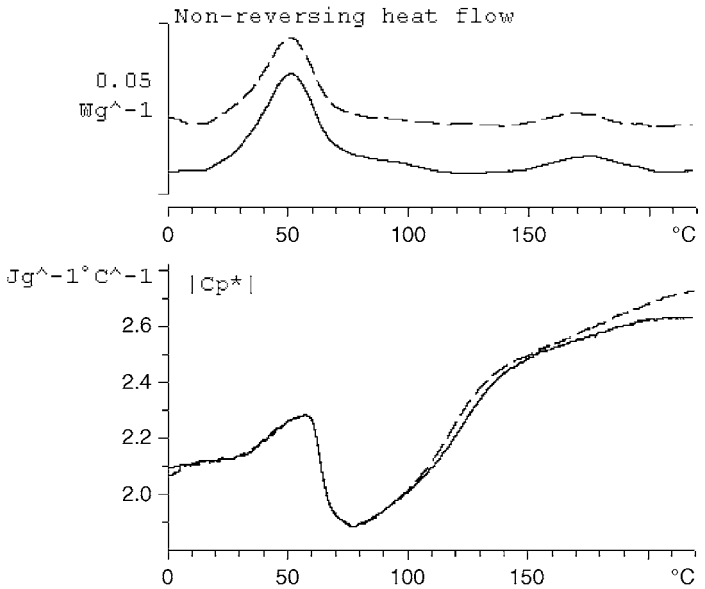

Fig. 5. Non-reversing heat flow and modulus of the complex heat capacity of samples A (solid line) and B (dashed line) of the non-isothermal cure of the DGEBA–3DCM system at an underlying heating rate of 0.1 K min^{-1}, an amplitude of 0.2 K and a period of 60 s. The scale of the specific heat flow is relative and the curves are shifted vertically for clarity.

260 °C at 10 K min^{-1}, the T_g rises to 143 °C in a final scan at the same heating rate.

3.3. Vitrification and devitrification

As mentioned above, the DGEBA–3DCM system shows vitrification and devitrification transitions during the curing within a wide interval of temperature. At temperatures close to −40 °C, the system shows the transition from the glassy to the liquid state of the unreacted system. The glass transition temperature of the unreacted system was measured by the $\langle\phi\rangle$ and $|C_p^*|$ signals. As mentioned above, the dynamic glass transition measured by $|C_p^*|$ is slightly higher than the thermal glass transition measured by $\langle\phi\rangle$. The average value of $T_{g0,|C_p^*|}$ is −39.3 °C, while the average value of $T_{g0,\langle\phi\rangle}$ is −42.5 °C. Both values of T_{g0} and the variation of $|C_p^*|$ at T_{g0} are shown in Table 1. The variation of $|C_p^*|$ at T_g is defined as

$$\Delta|C_p^*|(T_g) = |C_{p,l}^*| - |C_{p,g}^*| \quad (1)$$

where $|C_{p,g}^*|$ and $|C_{p,l}^*|$ are the extrapolated modulus of the complex heat capacity of the sample in the glassy and liquid state, respectively.

The analysis of the $|C_p^*|$ signal shows other transitions which correspond to the vitrification and further devitrification of the system. The T_g of the system increases during the non-isothermal curing and equals the curing temperature T_c. In this situation, the system vitrifies and the kinetics of curing becomes diffusion controlled. As a consequence of this kinetic change, the reaction rate slow down and the degree of conversion levels off. This process of vitrification is observed by the decay of the $|C_p^*|$ signal for a fixed frequency of modulation. The T_g of the system is higher than T_c during an interval of time, which depends on the heating rate. As faster is the heating rate the shorter is the interval of time that the system remains in the glassy state. As T_c increases, the T_g becomes lower than T_c and the system reaches the rubbery state. This process of devitrification is observed by an increase of the $|C_p^*|$ signal. In the present DGEBA–3DCM system, these transitions were shown for underlying heating rates equal to or lower than 0.5 K min^{-1}. Since no experiments were performed between 1 and 0.5 K min^{-1}, one cannot exclude that, at heating rates slightly higher than 0.5 K min^{-1}, these transitions may also appear. The intensity of these transitions, measured by the variation of $|C_p^*|$, namely $\Delta|C_p^*|(T_v)$ and $\Delta|C_p^*|(T_{dv})$, which are shown in Table 2, are lower than the corresponding $\Delta|C_p^*|(T_{g0})$ of the unreacted system.

Fig. 6 shows the variation of $|C_p^*|$ with the temperature for the different heating rates. It is observed that the vitrification transition is sharper than the devitrification transition, and correspondingly, the interval of temperatures of the vitrification is shorter than for the devitrification. As the heating rate decreases, the vitrification takes place at lower temperatures, and the degree of conversion also tends to be smaller. On the other hand, the temperature of the beginning of the devitrification changes smoothly. It is noted that the devitrification temperature does not correspond to the final T_g obtained in a second scan (T_{g2s}), performed

Table 2
Temperatures of vitrification (T_v) and devitrification (T_{dv}) measured on $|C_p^*|$ signal, and variation of $|C_p^*|$ at the transition for different heating rates[a,b]

q_0 (K min^{-1})	$T_{v,o}$ (°C)	$T_{v,m}$ (°C)	$T_{v,e}$ (°C)	$\Delta\|C_p^*\|(T_v)$ (J g^{-1} K^{-1})	$T_{dv,o}$ (°C)	$T_{dv,m}$ (°C)	$T_{dv,e}$ (°C)	$\Delta\|C_p^*\|(T_{dv})$ (J g^{-1} K^{-1})
0.5	96.7	103.4	108.0	0.08	113.2	120.8	130.7	0.10
0.4	93.0	97.3	102.1	0.12	110.1	121.5	131.3	0.13
0.25	77.5	83.2	88.5	0.30	111.0	122.3	134.0	0.23
0.1[c]	60.1	64.6	69.3	0.45	107.1	122.5	138.0	0.39
0.1[c]	60.0	64.5	68.9	0.45	102.5	120.0	133.8	0.42

[a] The modulation conditions were: amplitude of 0.2 K and period of 60 s.

[b] The suffixes o, m and e in the vitrification or devitrification temperature indicate the measurement on the onset, midpoint and endpoint temperatures.

[c] These values correspond to two different samples (named A and B in Fig. 5) measured at the same heating rate and modulation conditions.

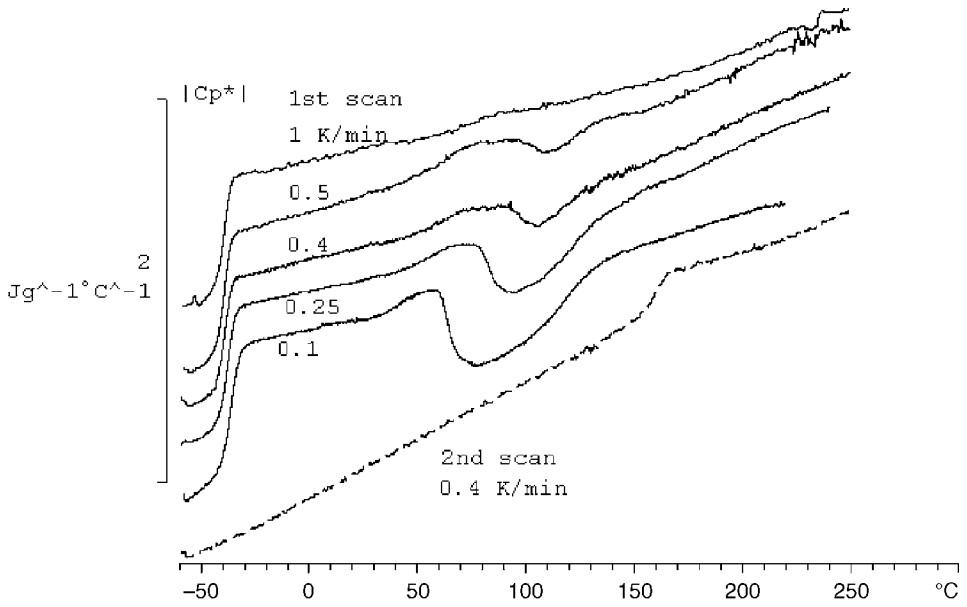

Fig. 6. Variation of the modulus of the complex heat capacity during the curing of the DGEBA–3DCM system at underlying heating rates of between 0.1 and 1 K min^{-1}. The $|C_p^*|$ measured in the second scan at 0.4 K min^{-1} is shown by the dashed line. Modulation conditions: an amplitude of 0.2 K and a period of 60 s. The scale of $|C_p^*|$ is relative and the curves are shifted vertically for clarity.

immediately after the first scan at the same q_0 and under the same modulation conditions. The values of the final T_g measured on $|C_p^*|$, namely $T_{g2s,|C_p^*|}$, shown in Table 1, are about 25 °C higher than the endset devitrification temperature $T_{dv,e}$ shown in Table 2. This difference is due to the aforementioned residual reaction that may take place after the devitrification up to the final temperature of the first scan, which is between 220 and 250 °C at heating rates of between 0.1 and 0.4 K min^{-1}, respectively.

At the same time, the effects of the vitrification and devitrification phenomena may be detected also in the phase angle signal. Fig. 7 shows the variation of the uncorrected phase angle with the temperature for the different heating rates. At the beginning of the scan, the relaxation associated with the glass transition of the unreacted system is clearly detected. The average peak temperature is -38.5 ± 0.8 °C, as shown by $T_{g0,\delta}$ in Table 1. At increasing temperatures, for q_0 of 0.5 and 0.4 K min^{-1}, vitrification and devitrification are shown as a broad peak. At the lowest heating rates of 0.25 and 0.1 K min^{-1}, a peak corresponding to the vitrification can be clearly observed close to a broader peak at higher temperatures, which is a consequence of the devitrification. Nevertheless, the measurement of this relaxation by the phase angle depends on the corrections that are mainly due to the change in the heat capacity and to the thermal conductance between the system sample-pan and the measuring thermocouples [15].

3.4. The glass transition temperature of the highly crosslinked resin

The final glass transition temperature of the resin was measured in a second scan immediately performed after the non-isothermal curing at the same heating rate and modulation conditions. The $|C_p^*|$ and phase angle signals obtained in this second scan at $q_0 = 0.4$ K min^{-1}, are shown in the bottom of Figs. 6 and 7, respectively. The modulation conditions were the same as in the first scan: an amplitude of 0.2 K and a period of 60 s. The $|C_p^*|$ signal shows the final glass transition of the resin at a temperature interval of between 151 and 166 °C and the phase angle shows the relaxation associated with this transition as a broad peak between 130 and 170 °C.

The values of $T_{g2s,|C_p^*|}$ measured on the $|C_p^*|$ signal at $q_0 \leq 0.4$ K min^{-1}, shown in Table 1, are between 156 and 159 °C with an average value of 158.1 °C. This value of T_g agrees very well with the average value of

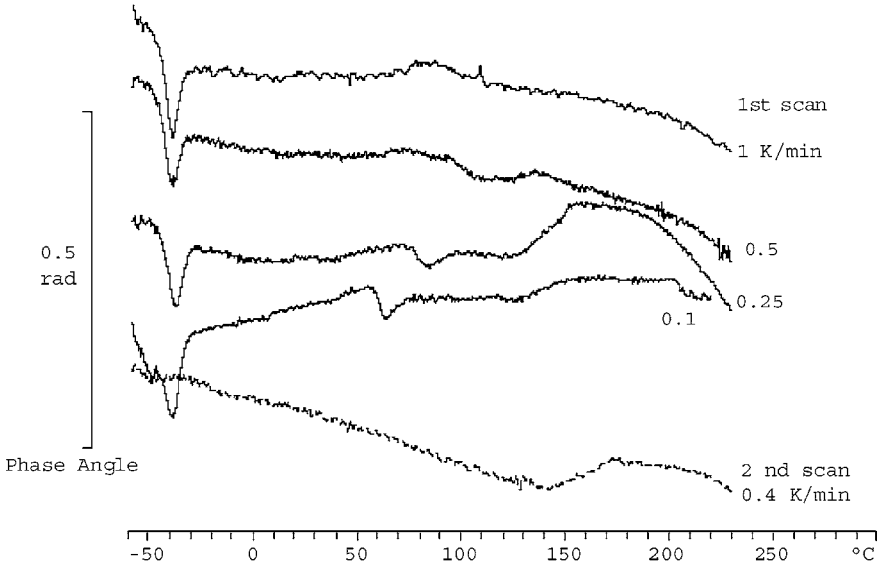

Fig. 7. Variation of the uncorrected phase angle during the curing of the DGEBA–3DCM system at underlying heating rates between 0.1 and 1 K min^{-1}. The phase angle measured in the second scan at 0.4 K min^{-1} is shown by the dashed line. Modulation conditions: an amplitude of 0.2 K and a period of 60 s. The scale of phase angle is relative and the curves are shifted vertically for clarity.

$T_{g,|C_p^*|} = 156.1 \pm 0.9$ °C, obtained at $q_0 = 1$ K min^{-1}, an amplitude of 0.5 K and a period of 60 s, in samples previously cured isothermally between 40 and 140 °C for different curing times, and subsequently postcured up to 270 °C under the aforementioned conditions [1]. The difference between the final T_g and the end temperature of the devitrification process confirms the difficulty to reach the completion of the reaction. At high degrees of crosslinking, the unreacted groups remain in spatially separated positions and, because of the high connectivity of the network, they are unable to meet and react. There is a topological restriction that prevents the obtention of the fully cured epoxy [17–20].

The final T_g of the samples cured at 1 and 0.5 K min^{-1}, shown in brackets in Table 1, are much lower than the other values, due to the samples being subjected to temperatures above the onset of the thermal degradation. In fact, the end temperature of the non-isothermal curing was 300 °C in both cases, and the onset of thermal degradation was 270 and 255 °C, respectively (Table 3). Under these conditions, the samples were submitted to the thermal degradation process for 30 and 90 min, in which they were heated at 1 and 0.5 K min^{-1}, respectively.

3.5. The continuous heating transformation cure diagram

The temperatures and times of the vitrification and devitrification transitions have been plotted in a CHT cure diagram as shown in Fig. 8. These points give the vitrification and devitrification lines (dashed lines) that meet on a heating rate line slightly higher than 0.5 K min^{-1}, probably about 0.6 K min^{-1}. Both lines delimit a region in which the reacting system remains in the glassy state. The points corresponding to the

Table 3
Thermogravimetric results on thermal degradation of the DGEBA–3DCM system at low heating rates: onset (T_{do}), onset extrapolated ($T_{do,e}$) and inflexion ($T_{d,inf}$) temperatures of thermal degradation

q_0 (K min^{-1})	T_{do} (°C)	$T_{do,e}$ (°C)	$T_{d,inf}$ (°C)
1	270	317.4	333.2
0.5	255	305.9	321.3
0.4	251[a]	296.8[a]	318.7[a]
0.25	250	290.9	312.6
0.1	220	264.4	293.8

[a] Temperatures estimated from the results obtained between 0.1 and 20 K min^{-1}. The results obtained at heating rates between 2.5 and 20 K min^{-1} were shown in Table 1 of [1].

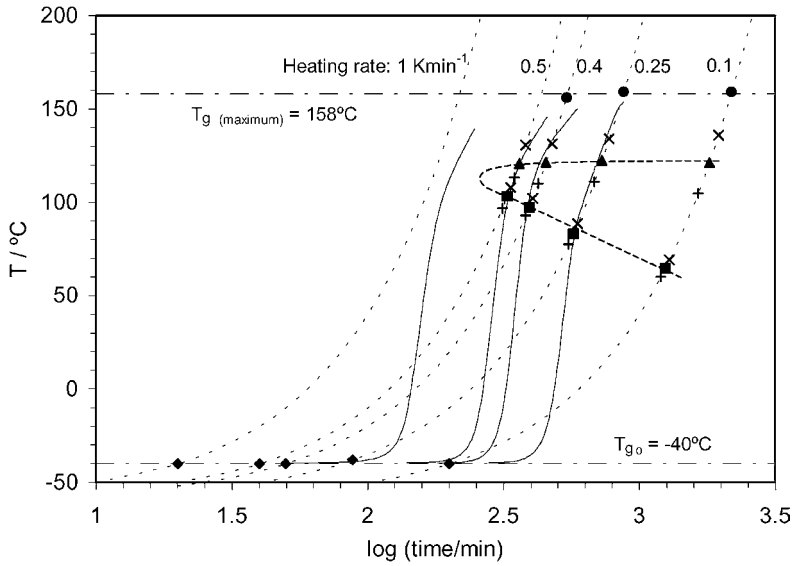

Fig. 8. CHT cure diagram of the DGEBA–3DCM system. The dotted lines show the indicated underlying heating rates. The filled squares and filled triangles correspond to the vitrification and devitrification temperatures, respectively. The onset and endset of the vitrification and devitrification are shown by the symbols (+) and (×), respectively. The dashed lines that connect the vitrification and devitrification points serve as a guide for the eye. The glass transitions of the unreacted system $T_{g0,|C_p^*|}$ (◆) and the maximum glass transition $T_{g2s,|C_p^*|}$ (●) are also indicated. The continuous lines show the dependence of T_g on the time for the indicated heating rates.

glass transition of the unreacted system and the final glass transition, both measured on $|C_p^*|$ signal, are also shown in this CHT diagram. It must be noted that the CHT diagram in Fig. 8 only shows experimental values and the vitrification line has not been completed at slower heating rates in order to show the typical sigmoidal shape presented in other works [2,3,7]. Furthermore, the diagram shows the interval of each transition, whereby the vitrification is shown by the midpoint (filled squares) but also by the onset (+) and endset (×) points. The midpoint devitrification is shown by filled triangles and the onset and endset are also shown by the same symbols as in the vitrification.

In other epoxy resins, the devitrification temperature is practically the same as the final glass transition temperature of the resin [2,3,7]; however, this is not the case with our epoxy. As was discussed in a previous section, our DGEBA–3DCM system displays a particular behaviour of crosslinking at high degrees, due to the steric hindrance of the methyl group, which inhibits the reaction of the hydrogens of the amine groups. In addition to this steric effect, we must add the difficulty of obtaining full conversion during the final stages of the reaction due to topological constraints [17–20]. Both effects prevent the maximum glass transition (named $T_{g\infty}$ by Gillham and co-workers [2,3,17]) from being achieved. A similar situation was shown in the time-temperature-transformation cure diagram of this system, shown elsewhere [1].

It is usual to complete the CHT cure diagrams with the T_g–t lines [2,3,7]. In order to draw these lines, a relation between the degree of conversion and the glass transition temperature of the system is required. This relation may be derived from experimental results obtained by the residual heat curing method. The values of the degree of conversion and the T_g measured at curing temperatures of 60, 90, 130 and 160 °C are shown in Fig. 9. A relationship between these two properties may be found by making use of the so-called DiBenedetto equation, which was reported by Nielsen [21], and subsequently modified by Pascault and Williams [22]:

$$\frac{T_g - T_{g0}}{T_{g\infty} - T_{g0}} = \frac{\lambda\alpha}{1 - (1-\lambda)\alpha} \quad (2)$$

where T_{g0} is the glass transition temperature of the unreacted system, $T_{g\infty}$ the maximum glass transition,

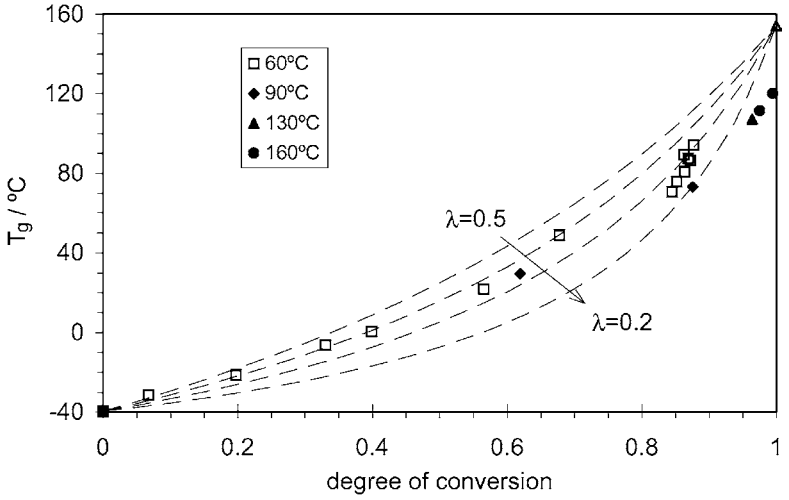

Fig. 9. Relation between the T_g and the degree of conversion for the DGEBA–3DCM system. The lines are fitted to the DiBenedetto equation for values of $T_{g0} = -40$ °C (■) and $T_{g\infty} = 154.3$ °C (△) and the parameter λ between 0.2 and 0.5. The symbols correspond to the samples cured at the indicated temperatures for different interval of times.

attained when $\alpha = 1$, and λ is an adjustable parameter between 0 and 1. Curves of T_g–α for values of λ between 0.2 and 0.5 calculated with $T_{g0} = -40$ °C and $T_{g\infty} = 154.3$ °C, which is the average value of the maximum T_g measured on $\langle\phi\rangle$ at 1 K min^{-1}, an amplitude of 0.5 K and a period of 60 s, are shown in Fig. 9. A good fit was observed for values of α up to 0.6–0.7 when λ is taken as 0.4. According to Pascault and Williams [22], the parameter λ may be identified with the ratio of the heat capacities $\Delta C_{p\infty}/\Delta C_{p0}$, resulting in our DGEBA–3DCM system a value of 0.38. Therefore, a good fit for $\lambda = 0.4$ is not surprising, since this is practically the value calculated from the heat capacities. Nevertheless, at $\alpha > 0.7$ a deviation from the fit is observed. This deviation is attributed to the under-estimation of the residual heat of curing, which gives higher values of α.

The values of the degree of conversion, shown in Fig. 4, may be converted to the T_g, which corresponds to this conversion, by using the relationship α–T_g from Eq. (2). The results obtained for the heating rates of between 0.25 and 1 K min^{-1} are shown in Fig. 8. At a heating rate of 1 K min^{-1}, the T_g–t line (continuous line) always lies under the T–t line (dotted line), and no vitrification is detected. However, at lower heating rates, the T_g–t line crosses the T–t line at a point close to the vitrification point, where $T_g = T$, and subsequently crosses the T–t line again at the devitrification point. Taking into account the particularities found in the determination of the T_g in the highly crosslinked resin and the determination of the degree of conversion of the DGEBA–3DCM system, the agreement between the previously determined points of vitrification and devitrification and the crossing points is acceptable. The T_g–t line at 0.1 K min^{-1} is not shown in Fig. 8 due to the double step of the curve α–T, which do not allow the use of the single T_g–α relation of Eq. (2).

4. Conclusions

The non-isothermal cure of an epoxy resin based on DGEBA with a diamine based on 3DCM was analysed by TMDSC at underlying heating rates of between 0.1 and 1 K min^{-1}, and modulation conditions of 0.2 K amplitude, and a period of 60 s. The heats of curing measured by the total heat flow at these low heating rates are slightly higher than those determined by conventional DSC.

The use of heating rates lower than 0.5 K min^{-1} allows the observation of the vitrification and devitrification processes in the complex heat capacity signal. The temperature of the vitrification tends to decrease when q_0 decreases, whereas the temperature of devitrification practically has no variations. Both

temperatures of vitrification and devitrification were used to delimit a glassy zone in the CHT cure diagram. In this DGEBA–3DCM system, different values between the end temperature of devitrification and the final T_g of the resin were observed. This effect is due in part to the steric hindrance between the amine and the methyl groups of the hardener, which inhibits the reaction of the secondary amine, and also to the topological constraints that add more difficulties to the reaction of these groups at high degrees of crosslinking.

The total heat flow shows a main peak followed by a very broad peak of low intensity, which is a consequence of the diffusion controlled step detected in the $|C_p^*|$ signal. However, at 10 K min^{-1} an additional peak of very low intensity appears between 150 and 200 °C, which may be due to a residual curing of the epoxy with the amine groups.

The CHT diagram may be completed by the T_g–t lines, which give the evolution of the T_g of the system with the time for different heating rates. The calculation of these lines is performed from the relation between T_g and the degree of conversion. Nevertheless, the calculation of the degree of conversion is subjected to some uncertainty due to its dependence on both the baseline type and the limits selected in the integration of the heat of curing. Furthermore, in the DGEBA–3DCM system, the aforementioned effect of steric hindrance introduces deviations in the relationship between T_g and α by a DiBenedetto type equation. Both effects give some deviations in the coincidence of the T_g–t and T–t lines in the corresponding vitrification and devitrification points.

Acknowledgements

Financial support has been provided by CICYT (MAT97-0634-C02-02 and MAT2000-1002-C02-01). The authors are grateful to CIBA Speciality Chemicals for supplying the epoxy and the hardener.

References

[1] S. Montserrat, J.G. Martín, J. Appl. Polym. Sci. (2002), in press.
[2] G. Wisanrakkit, J.K. Gillham, J.B. Enns, J. Appl. Polym. Sci. 41 (1990) 1895.
[3] G. Wisanrakkit, J.K. Gillham, J. Appl. Polym. Sci. 42 (1991) 2453.
[4] M. Reading, Trends Polym. Sci. 1 (1993) 248.
[5] G. Van Assche, A. Van Hemelrijck, H. Rahier, B. Van Mele, Thermochim. Acta 286 (1996) 209.
[6] G. Van Assche, A. Van Hemelrijck, H. Rahier, B. Van Mele, Thermochim. Acta 304/305 (1997) 317.
[7] A. Van Hemelrijck, B. Van Mele, J. Therm. Anal. 49 (1997) 437.
[8] S. Swier, G. Van Assche, A. Van Hemelrijck, H. Rahier, E. Verdonck, B. Van Mele, J. Therm. Anal. 54 (1998) 585.
[9] H.J. Flammersheim, J. Opfermann, Thermochim. Acta 337 (1999) 141.
[10] S. Montserrat, Y. Calventus, P. Colomer, USER COM 11 (2000) 17.
[11] W.R. Ashcroft, in: B. Ellis (Ed.), Chemistry and Technology of Epoxy Resins, Chapman and Hall, Glasgow (Chapter 2) 1996.
[12] S. Montserrat, I. Cima, Thermochim. Acta 330 (1999) 189.
[13] J.M. Hutchinson, S. Montserrat, Thermochim. Acta 304/305 (1997) 257.
[14] J.M. Hutchinson, S. Montserrat, Thermochim. Acta 377 (2001) 63.
[15] J.E.K. Schawe, Thermochim. Acta 361 (2000) 97.
[16] D. Verchère, H. Sautereau, J.P. Pascault, C.C. Riccardi, S.M. Moschiar, R.J.J. Williams, Macromolecules 23 (1990) 725.
[17] G. Wisanrakkit, J.K. Gillham, J. Coatings Tech. 62 (1990) 35.
[18] A. Hale, Ch.W. Macosko, H.E. Bair, Macromolecules 24 (1991) 2610.
[19] E.F. Oleinik, Adv. Polym. Sci. 80 (1986) 49.
[20] S. Montserrat, J. Therm. Anal. 40 (1993) 553.
[21] A.T. DiBenedetto, L.E. Nielsen, J. Macromol. Sci. Rev. Macromol. Chem. C3 (1969) 69.
[22] J.P. Pascault, R.J.J. Williams, J. Polym. Sci. Polym. Phys. 28 (1990) 85.